Journal of
BIOPHOTONICS

FULL ARTICLE

In-vitro analysis of early calcification in aortic valvular interstitial cells using Laser-Induced Breakdown Spectroscopy (LIBS)

Seyyed Ali Davari[+,1,2] *Shirin Masjedi*[+,2] *Zannatul Ferdous*,[2] *and Dibyendu Mukherjee*[*,1,2]

[1] Nano-BioMaterials Laboratory for Energy Energetics & Environment (nbml-E³), University of Tennessee, Knoxville, TN 37996, USA
[2] Department of Mechanical, Aerospace and Biomedical Engineering, University of Tennessee, Knoxville, TN 37996, USA
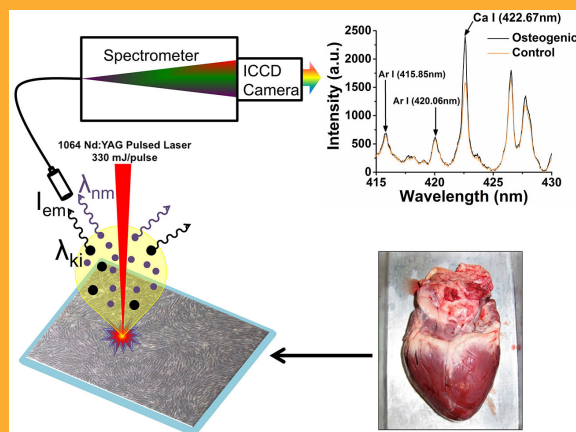
Calcific aortic valve disease (CAVD) is a major cardiovascular disorder caused by osteogenic differentiation of valvular interstitial cells (VICs) within aortic valves. Conventional methods like colorimetric assays and histology fail to detect small calcium depositions during *in-vitro* VIC cultures. Laser-induced breakdown spectroscopy (LIBS) is a robust analytical tool used for inorganic materials characterizations, but relatively new to biomedical applications. We employ LIBS, for the first time, for quantitative *in-vitro* detection of calcium depositions in VICs at various osteogenic differentiation stages. VICs isolated from porcine aortic valves were cultured in osteogenic media over various days. Colorimetric calcium assays based on arsenazo dye and Von Kossa staining measured the calcium depositions within VICs. Simultaneously, LIBS signatures for Ca I (422.67 nm) atomic emission lines were collected for estimating calcium depositions in lyophilized VIC samples. Our results indicate excellent linear correlation between the calcium assay and our LIBS measurements. Furthermore, unlike the assay results, the LIBS results could resolve calcium signals from cell samples with as early as 2 days of osteogenic culture. Quantitatively, the

LIBS measurements establish the limit of detection for calcium content in VICs to be ~ 0.17 ± 0.04 μg which indicates a 5-fold improvement over calcium assay.

Picture: Quantitative LIBS enables *in-vitro* analysis for early stage detection of calcium deposition within aortic valvular interstitial cells (VICs).

* Corresponding author: e-mail: dmukherj@utk.edu, Tel: 865–974-5309, Fax: 865–974-5274
+ First co-authors

1. Introduction

Calcific aortic valve disease (CAVD) is a common cardiovascular disorder affecting 25 % of the elderly population over the age of 65 and at severe stages, 4 % over the age of 80 [1,2]. Early detection of CAVD is elusive and late detection of CAVD leaves the patients with the only viable treatment of aortic valve transplant surgery [3,4]. Early stage CAVD is associated with calcium (Ca) accumulation in aortic valves that can lead to stenotic aortic valves wherein extracellular matrix (ECM) decomposition and tissue stiffening occurs along with large nodule formation within the aortic valve cusps [5]. CAVD is an active cell-mediated condition, where the inhabitant valvular interstitial cells (VICs) differentiate into osteoblast-like cells and exhibit bone-like characteristics, such as calcific nodule formation [6,7], hydroxyapatite deposition [2,8] and osteogenic marker expressions [9–11].

Typically computer tomography (CT) and echocardiography are used as the dominant tools for clinical diagnosis of CAVD in patients [12–14]. For direct evaluation of aortic valve calcification for research purposes, various techniques have been developed to measure the calcium deposition in VICs or valve tissue sections on a laboratory platform. The most common techniques include Von Kossa staining [6,15], Alizarin Red staining [15], Raman spectroscopy, scanning electron microscopy (SEM) [16], transmission electron microscopy (TEM) [16], atomic absorption spectroscopy [17], arsenazo III calcium assay [15], and o-cresolphthalein complexone calcium assay [18] measurements. However, till date, these *in-vitro* methods have not been able to demonstrate the limits of detection (LOD) needed to quantify calcium depositions in significantly low amounts during the early onset of calcification in aortic valves. Calcium quantification through histology is time-consuming and lacks accuracy due to false positive stained regions in image analysis. The spectroscopy methods used for calcium detection in calcified aortic valve tissues, including near-infrared (NIR) Raman [19], Fourier transform infrared (FTIR) [20] and atomic absorption [21] are all sensitive quantification techniques for calcium. However, NIR Raman can be prone to false positive results due to the heterogeneity of human tissue and high dependency on chemical band positions. On the other hand, FTIR is typically unable to quantify calcium contents within the aortic valves. Additionally, atomic absorption spectroscopy is limited to tissue sections and is an expensive technique [22]. Thus, there exists a critical need for robust *in-vitro* analytical techniques that can achieve rapid and highly accurate detection of extremely small calcium depo-

sitions in VICs with minimal sample preparation steps. In turn, such analytical advancements can expedite biomedical research in diagnosing the elusive origins of enhanced CAVD.

Laser Induced Breakdown Spectroscopy (LIBS) is a relatively non-destructive spectrochemical characterization technique, which can address the aforementioned issues in a facile, yet effective manner. Typically, LIBS involves the collection and processing of optical emissions emanating from a high-irradiance pulsed laser tightly focused to generate a high temperature, high pressure micro-plasma containing the analyte of interest [23]. These emissions (ionic, atomic and molecular), collected as spectral signatures, can reveal the constituents and properties of the plasma and hence, the sample. The relatively simple set-up and minimal sample preparations for LIBS have drawn the attention of analytical researchers in recent years [24]. Additionally, the fast and easy operation, and data collection make LIBS ideal for in-situ applications [25].

In the past, LIBS has found a vast amount of applications in diverse spectral, and elemental studies ranging from combustion [26–28], and environmental/bio-hazard analysis [29–33], to forensics[34], explosives detection [35–37], pharmaceutical [38,39] and biomedical [40,41] applications. Specifically, our recent application of calibration-free quantitative LIBS towards metal nanoparticles, carbonaceous aerosols and nanoalloy characterizations has established the technique at the forefront of elemental analysis in complex matrices [25,31,42]. In biological applications of LIBS, Hybl [43] showed the capability of LIBS as a bioaerosol classifier to distinguish different classes of biological agents using Principal Component Analysis (PCA). Kumar [40] introduced LIBS as an automated, real-time technique for cancer diagnosis based on the differences in the trace element concentrations in normal and malignant cells. A recent study has also used LIBS signatures resulting from tissue ablation to distinguish porcine gland from nerve tissues in order to create a feedback control mechanism during real-time laser surgery [44]. In regards to the application of quantitative LIBS for biological and biomedical studies, Samek [45] resorted to tissue-equivalent synthetic pellets of $CaCO_3$ as the external reference matrix to establish standard calibration curves for quantitative analysis of toxic elements in calcified hard tissue samples. The complexity of laser-sample interactions has mostly restricted the LIBS applications for calcified biological samples to quantitative elemental analysis of hard calcified tissues such as teeth, and bones [45,46]. To this end, the commonly employed technique of lyophilization could possibly provide a solution for removing the moisture from the soft tis-

sue samples without altering the biological structures. But, to the best of our knowledge, no report exists on the use of LIBS to quantify calcifications in lyophilized VICs without any external calibration standard.

In this study, we establish LIBS for the first time as a quantitative analytical technique for *in-vitro* analysis of calcium depositions in VICs subjected to osteogenic culture over 2 to 21 days. The appearance of calcium deposits within the matrix is a sign of osteoblastic shift in valvular cells. Early diagnosis of CAVD demands fundamental research that can enable laboratory-based rapid screening and analyses of early calcification in VICs to understand the initiation and origin of the disease. For that, VICs behavior should be studied over time from normal to calcified conditions. Our goal was to identify the earliest time that the cultured VICs start to show any calcium depositions. Specifically, we investigate the evolution of the calcium atomic emissions for Ca I (422.67 nm) from LIBS measurements on the aforesaid VIC samples. Our results for the spectral signatures of Ca will be compared and correlated to calcium assays to demonstrate the efficacy of LIBS in quantifying the amount of calcium depositions in VICs. The LODs for both methods will be compared to establish the high-resolution capabilities of LIBS over the assays in detecting early-stage calcification in aortic valve cells.

2. Materials and methods

2.1 VIC isolation and culture

VICs were isolated from porcine aortic valve cusps (Wampler's Farm Sausage, Inc., Lenoir City, TN) by collagenase II digestion, as previously described [6], and cultured in growth media (DMEM, 10 % FBS, 1 % L-glutamine, and 1 % Penicillin/Streptomycin) at 37 $^{\circ}$C and 5 % CO_2 until four passages.

Unless otherwise specified, the VICs were seeded at a density of 250,000 cells/well into 6-well plates. To stimulate calcification on VICs, osteogenic media consisting of 2.18 g/L beta-glycerophosphate, 50 mg/L L-ascorbic acid 2-phosphate and 1 mM dexamethasone (all purchased from Sigma, St. Louis, MO) in regular media was added to the experimental samples. Control samples were cultured in regular media under similar condition. The media was changed every 2 days. Experiments were performed after 2, 4, 7, 10, 14 and 21 days of VIC culture in osteogenic media.

2.2 Lyophilization

VIC samples were freeze-dried prior to being used for LIBS quantification. At each time-point, the VIC monolayer was washed with phosphate-buffered saline (PBS). Then, the cells were removed from the well surface by scraping and transferred to silicon wafer substrates (rectangular, $\sim 1 \times 1$ cm^2). Subsequently, the VICs were frozen at -20 $^{\circ}$C for at least 8 hours and then lyophilized overnight.

2.3 DNA content measurement

A fluorescence DNA assay was used to measure the cell density of the VIC samples [6, 47]. The VICs were scraped and digested in Proteinase-K solution (1 mg/mL) (Sigma). Then, the cell lysates were incubated in a water bath for 90 minutes at a temperature between 60–70 $^{\circ}$C and then heated at >70 $^{\circ}$C for 30 minutes to denature the Proteinase-K. Hoechst 33258 dye (Sigma) was used to tag the released DNA and fluorescence emission was measured using a BioTek H1 plate reader at 458 nm. Calf thymus DNA standards (Sigma) were used in each assay to calculate DNA density.

2.4 Calcium assay

A colorimetric calcium assay based on arsenazo dye was used to measure the calcium content of the osteogenic VICs [6]. First, VICs were homogenized in 1N acetic acid, then arsenazo dye was added to the samples. The calcium content was measured against calcium standard (Ricca chemical, Arlington, TX). Samples absorbance was detected at 650 nm using a BioTek H1 plate reader. The calcium content was normalized to total DNA content.

2.5 Von Kossa staining

Von Kossa staining was used to determine the amount of calcium deposition [6]. The VICs in each well were fixed in 10 % formalin (Fisher Scientific, Fair Lawn, NJ). After washing with distilled water for 3 times, a silver nitrate (Ricca Chemical Co., Arlington, TX) solution (3 %) was added to the fixed VICs. Then the samples were incubated and exposed to UV until the calcium salts turned dark brown or black. The undissolved salts were removed using a 5 % sodium thiosulfate (Sigma) solution and dehydrated with Flex before imaging. 10X images of the calcific depositions were obtained with a bright

field microscope (Motic Inc., BC, Canada), and ImageJ software (NIH) was used for image analysis.

2.6 LIBS setup and measurement

The LIBS experimental set-up is illustrated in Figure 1. A Q-switched Nd-YAG pulsed laser with a nominal wavelength of 1064 nm operating at 200 mJ/pulse, and a pulse width of 8 ns (Make: Insight 122551-R) was used to generate the laser-induced plasma. The irradiance was focused with a 25 mm diameter fused silica lens, with a focal length of 35 mm, which provides ~10–15 GW/cm^2 flux approximately at the focal point. The spot size on the sample was set to be 75 μm in diameter. In order to improve the stability of the plasma and reduce the self-absorption of the emissions, a mixture of argon (1 lpm) and helium (3 lpm) was used as the buffer gas during the experiments.

The plasma emissions are collected with a fiber optic at 45 degree angle, which allows the collection of the optimum intensity from the plasma volume. The collected emissions are directed through a fiber optic to a Czerny-Turner spectrometer (Make: Andor Technology; Model: Shamrock - SR-303i-A) with 1200 grooves/mm grating (resolution ~ 0.1 nm at 500 nm and nominal dispersion ~2.58 nm/mm). The spectrometer slit width was fixed at 100 μm for all experiments reported here in order to have the optimum spectral line intensity and resolution. A time-gated intensified charge-coupled device (ICCD) detector array (1024 × 1024 CCD) (Make: Andor Technology; Model: DH334T-18U–E3) records the spectral lines at the spectrometer exit focal plane. The time gating is synchronized with the laser Q-switch.
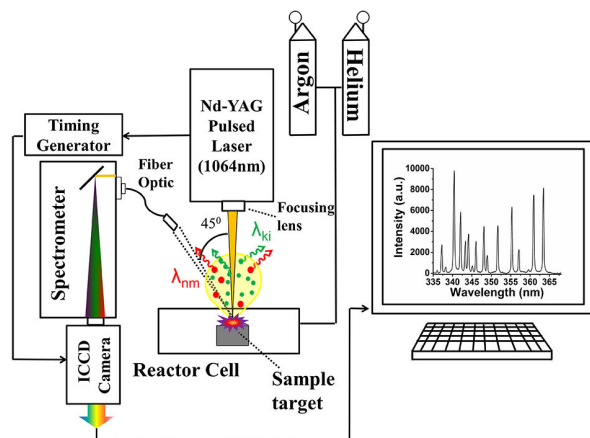
Figure 1 Schematic for the experimental set-up of LIBS.

Calcium atomic emission line was chosen from NIST Atomic Energy Levels Data Center [48]. Based on the emission strength, accuracy, and high transition probability, calcium atomic emission Ca I (422.67 nm) was chosen. In order to maximize the detection and sensitivity of the instrument, the sample emissions were recorded at different gate delays. At each gate delay, signal-to-noise ratio (SNR) was calculated by dividing the peak signal value measured at the wavelength of interest by the noise of the spectra. The noise was defined as the root mean square over the baseline (~40 pixel) adjacent to the analyte peak. The SNR was subsequently used as the effective emission (I_{em}) for all our spectrochemical data, and the optimal gate delay was determined from the maximum effective emission in time. For all quantitative comparisons of the LIBS spectral results, atomic emissions for Ca I (422.67 nm) from VICs in osteogenic culture were normalized by the respective emissions from the control cell samples.

2.7 Statistical analysis

Each experiment was repeated for three different cell isolations (n = 3). Statistical significance for different experiments was obtained using single-factor ANOVA. A p-value of ≤ 0.05 was considered significant. For LIBS measurements 50 different spots were collected for each sample, and the SNRs were calculated for each individual shot. The averaged SNR values over the 50 shots are reported here for each sample.

3. Results and discussion

3.1 Calcium assay

Colorimetric calcium assay results show that the calcium content of VICs cultured in osteogenic media increases overtime wherein after 14 and 21 days of osteogenic culture, the calcium content is significantly increased compared to the VICs at day 10 of osteogenic culture (Figure 2a). Moreover, the calcium fold changes (calcium content normalized to respective controls) are significantly elevated in VICs after 14 days of culture in osteogenic media (Figure 2b). However, for smaller amounts of calcium, the assay results have observable fluctuations between experimental and control VICs at day 4 and are unable to detect the calcium content at day 2 (Figure 2a). Similarly, analysis of calcium deposition among VIC monolayers by Von Kossa staining show increased calcification overtime (Figure 3a).
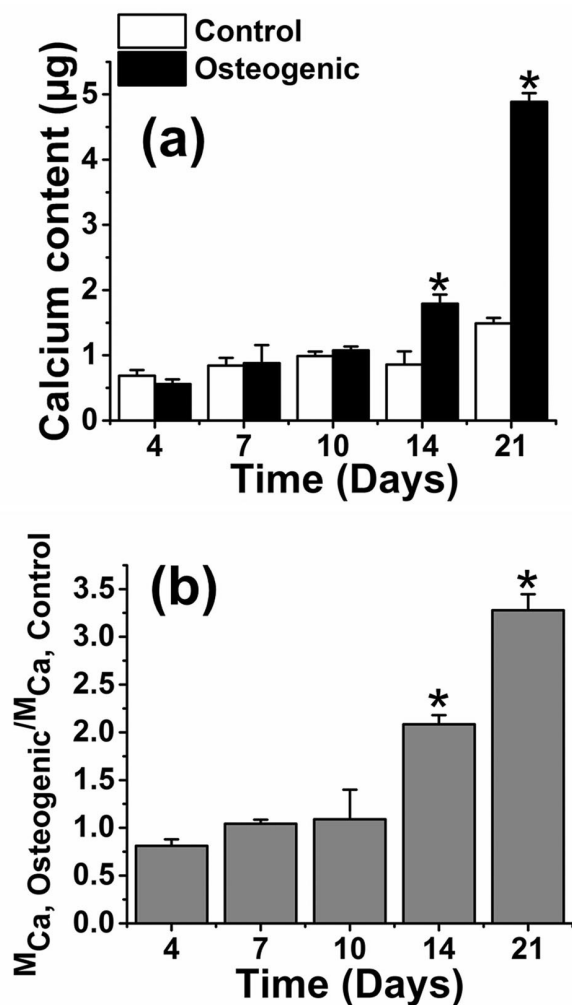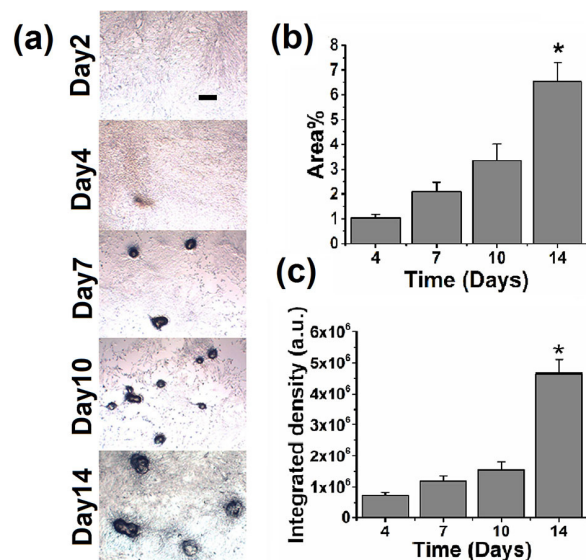
Figure 2 (a) Calcium assay results for control and osteogenic VICs after 4, 7, 10, 14 and 21 days of culture in osteogenic media, *p < 0.05 compared to osteogenic day 10 (b) normalized calcium content of osteogenic VICs to respective controls at each time point. The data represents mean ± std.error, n = 3 porcine aortic valves, *p < 0.05 compared to respective control.

Figure 3 (a) Von Kossa staining of VICs cultured in osteogenic media for 2, 4, 7, 10 and 14 days; the scale bar is 250 μm. Image analysis results showing (b) area percentage (c) integrated density of the calcium deposition within VICs cultured in osteogenic media for 4, 7, 10 and 14 days. The data represents mean ± std.error, n = 3 porcine aortic valves, *p < 0.05.

The representative images of calcium deposition in Figure 3a shows the nodules within VICs cultured in osteogenic media at different time points. It is obvious that at day 2 of osteogenic culture, no calcium deposition can be observed. Image analysis results demonstrate significantly elevated area percentage covered with calcium deposition and integrated density in VICs cultured in osteogenic media at day 14 as compared to the corresponding values over 4–10 days (Figure 3b, c).

Osteogenic differentiation of the VICs cultured in osteogenic condition advances over time and can be evaluated by change in the identified osteogenic markers. In a study on rat VICs cultured in osteogenic media for 7 and 14 days, the amounts of osteogenic markers increased significantly at day 14 compared to day 7, showing that longer duration of culture is associated with increased calcification [49]. Our calcium assay results are consistent with previous studies showing that amount of calcium increases over the time range of 4 to 21 days.

3.2 LIBS measurements

Representative LIBS spectra for Ca I (422.67 nm) atomic emission lines from VIC samples at day 10 collected over various gate delays are shown in Figure 4. It can be observed that the emission intensity of the 422.67 nm line decreases in time as a result of the diminishing continuum spectral background due to the recombination of free ions with electrons within the plasma that finally leads to atomic transitions from electronically excited to ground state. The temporal decrease in the absolute line intensity is accompanied by the respective decrease in the noise that results in an optimal gate delay wherein the analyte signal is relatively high as compared to the continuum noise in the spectrum. The temporal variations in signal-to-noise ratio (SNR) for the Ca I (422.67 nm) line, as
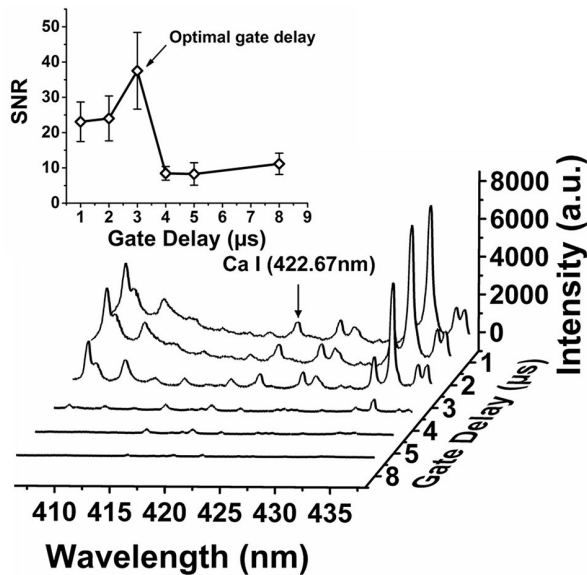
Figure 4 Representative LIBS spectra at different gate delays for Ca I (422.67 nm) emission lines from day 10 osteogenic VIC samples. (Inset: Temporal variations in SNR for Ca I line indicating optimal gate delay 3 μsec).

shown in the inset in Figure 4, indicates the optimal SNR to be 3 μs. Therefore, for all quantitative analysis presented here, we use a gate delay of 3 μs and a gate width of 5 μs for the Ca I (422.67 nm) detections in the VIC samples. The spectral signatures from osteogenic VICs cultured over days 2 to 21 are illustrated in Figure 5a indicating an increase in Ca I (422.67 nm) peak over time due to increasing calcium contents. The extent of calcification can be inferred by comparing the respective spectral signatures from osteogenic and control VICs, as indicated in Figure 5b for the specific case of osteogenic VICs cultured over 21 days. It is observed that except for the specific emission peak of Ca I (422.67 nm), both the control and analyte spectra demonstrate comparable emissions for the spectral signatures from the background Ar gas over the wavelength window of interest. This confirms that the spectral enhancement in the analyte line of interest (422.67 nm) arises specifically from the relevant differences in the calcium content between the control and osteogenic VICs, and is not an experimental artifact due to shot-to-shot fluctuations.

The evolution of the effective LIBS emissions (SNR) from both control and osteogenic VICs cultured over the 2 to 21 days are shown in Figure 6a. The slight variations in the SNR values for the control VIC samples over time can be attributed to shot-shot variations, especially considering the fact that the respective SNRs for the osteogenic VICs indicated consistently higher and temporally increasing values. The
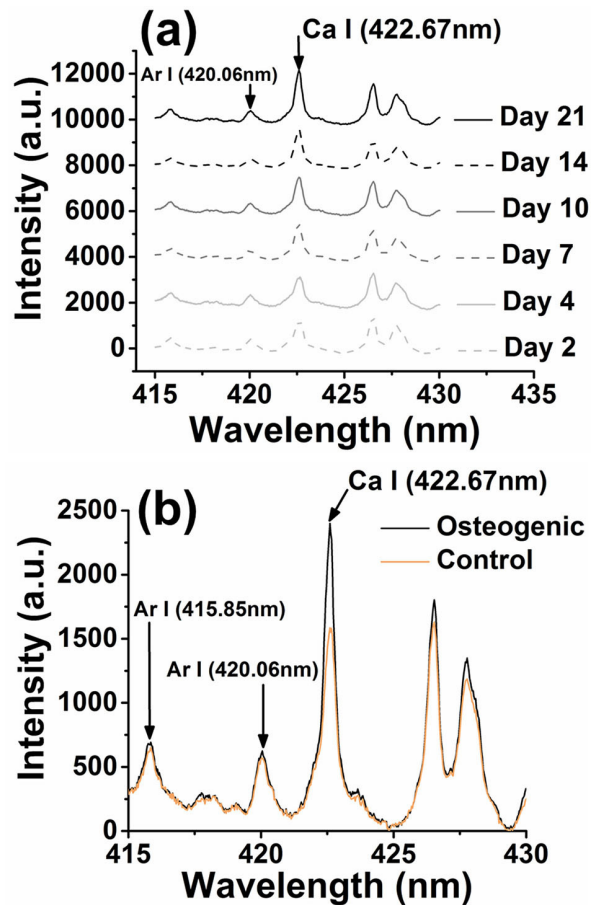

Figure 5 (a) LIBS signatures for Ca I (422.67 nm) emission line from osteogenic VICs at various time points of cell culture (spectra are shifted for better visualization); (b) Comparison of Ca I (422.67 nm) emissions from osteogenic and control VICs at day 21.

effective LIBS signal is proportional to the atomic number densities of calcium in the plasma volume as per the Maxwell-Boltzmann relations:

$$I_{em} \propto N_i \exp\left(\frac{\Delta E_{ki}}{k_B T_{exc}}\right)$$

where ΔE_{ki} is the energy difference between the transition states, and T_{exc} is the plasma temperature. Hence, the differences in the effective signals from the control and osteogenic VICs can be directly correlated to the differences in the relative calcium contents in the respective VIC samples. To account for the artifacts arising from spectroscopic, optical and experimental factors affecting the measured relative emission intensities at different conditions of the plasma evolution, Figure 6b indicates the effective signals from osteogenic VICs normalized to the
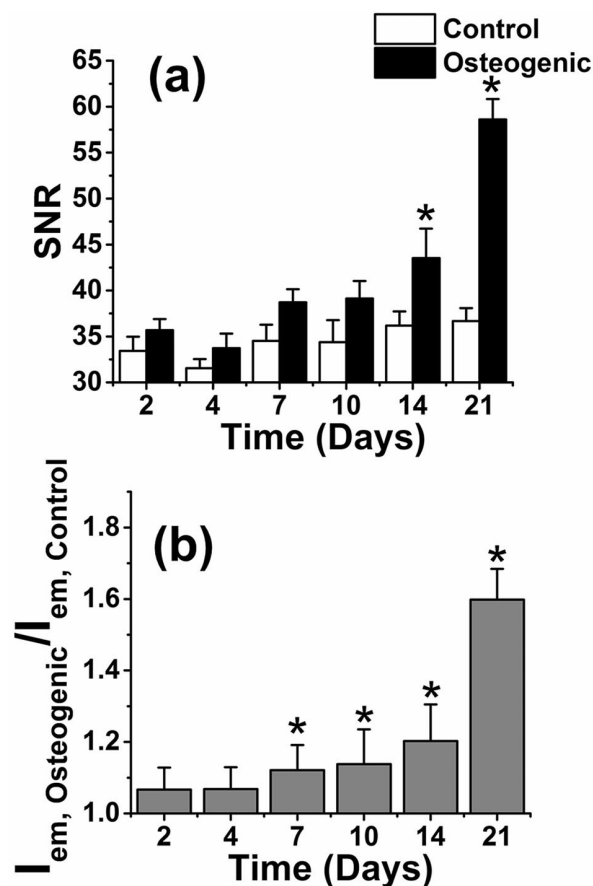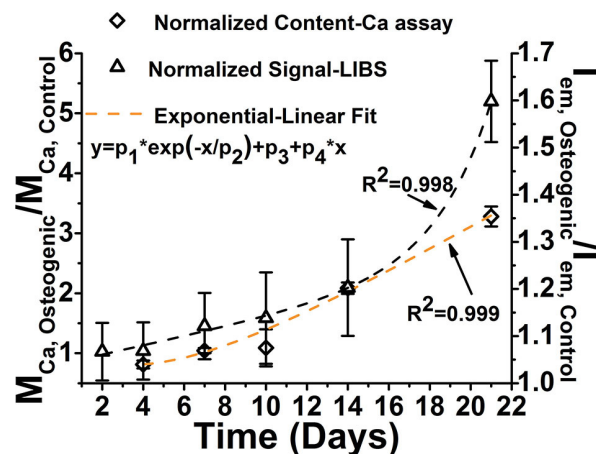
Figure 6 (a) LIBS results for control and osteogenic VICs after 2, 4, 7, 10, 14 and 21 days of culture in osteogenic media, p* < 0.05 compared to osteogenic day 10 (b) normalized calcium content of osteogenic VICs to respective controls at each time point. The data represents mean ± std.error, n = 3 porcine aortic valves, *p < 0.05 compared to respective control.

and b). On the other hand, the calcium assay fails to indicate any detectable signal above the background fluctuations for the VICs cultured up to day 7 (specifically, $M_{Ca, osteogenic}/M_{Ca, control} < 1$ for day 4 in Figure 2b). Additionally, neither the calcium assay nor the Von Kossa staining is able to detect any calcium deposition within osteogenic VICs after 2 days of culture. This indicates the inadequacy in the detection limits of the calcium assay. However, a greater sensitivity and superior detection limits of LIBS enable us to detect spectrally significant calcium signals from VIC samples with as early as 2 days of cell culture.

3.3 Time evolution and calibration curves based on calcium assay and LIBS measurements

A time evolution curve, as shown in Figure 7, is established for both normalized LIBS signals (from Figure 6b) and assay measurements (from Figure 2b) for the calcium contents in the osteogenic VIC samples. Fitted curves for both the aforementioned normalized data indicate a linear increase up to day 14 of VIC osteogenic culture which is subsequently followed by an exponential increase until day 21 (Figure 7 indicates the linear-exponential fit used). Therefore, one can observe a direct correlation between the calcium signal measurements from LIBS and calcium deposition detections

respective signals from the control samples ($I_{em, osteogenic}/I_{em, control}$) at 3 μs for the different days of cell culture. For each osteogenic VIC sample, the $I_{em, osteogenic}/I_{em, control}$ ratios in Figure 6b are proportionately higher than unity for the different days of culture, thereby confirming the excess calcium contents in osteogenic VICs over their respective controls. These results are even consistent over the early stages of calcifications (i. e., the samples cultured for 2 to 4 days). This definitely supports our hypothesis that the cultured VICs deposit elevated amounts of calcium as compared to their respective controls over all stages of osteogenic differentiation. In turn, these results point towards the ability of LIBS to resolve the onset of calcium depositions in early-stages of osteogenic differentiation ($I_{em, osteogenic} > I_{em, control}$ for both day 4 and day 7 VIC samples in Figure 6a

Figure 7 Time evolution curve for the normalized LIBS signal intensities ($I_{em, osteogenic}/I_{em, control}$; right y-axis) and assay measurements ($M_{Ca, osteogenic}/M_{Ca, control}$; left y-axis) for calcium contents in the osteogenic VIC samples indicating the similar linear-exponential trends for calcium depositions over the different periods of cell culture. (Fit equation as shown in the plot).
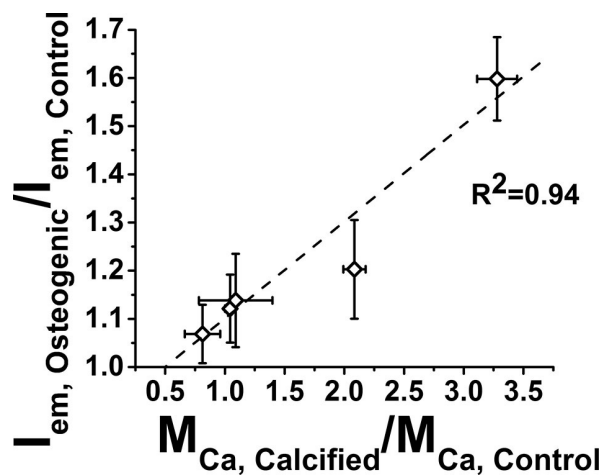
from calcium assay. To this end, Figure 8 establishes the linearity ($R^2 = 0.94$) in the correlation curve between normalized Ca signal emissions from LIBS ($I_{em, osteogenic}/I_{em, control}$) and calcium contents from calcium assay ($M_{Ca, osteogenic}/M_{Ca, control}$). It should be noted that the day 4 calcium assay data from Figure 2a indicate lower calcium content in the osteogenic VICs as compared to the respective controls. This is highly unlikely since it contradicts our very hypothesis that the cultured VICs deposit elevated amounts of calcium as compared to their control cell counterparts over all stages of osteogenic differentiations. Therefore, we infer that day 7 is the earliest time point during the cell culture durations in our study that allows for conclusive measurement of calcium content by calcium assay. In this context, the LOD for the assay measurements at day 7 is estimated to be ~0.84 µg. Our LOD from calcium assay measurements is relatively smaller or in the similar range as compared to previous studies using calcium assay approach that reported LODs of 1.5 [50], 50 [51], and 0.9 µg [52] for measured calcium contents in marrow stromal cells, vascular smooth muscle cells and mesenchymal stem cells respectively. In contrast, the normalized calcium signals measured by LIBS is observed to be greater than unity for all VIC samples even at time points as early as 2 and 4 days of culture. To this end, we quantitate our current LIBS analysis via LOD measurements from the calibration curve in Figure 9 that relates the detectable calcium assay measurements over 7 to 21 days to the corresponding LIBS calcium signals. We adopt the following definition of LOD here:

$$LOD = \frac{3\sigma_B}{S}$$

where, σ_B is standard deviation of the background of spectra and S is the slope of the linear fit to the calibration curve as shown in Figure 9. The calibration curve shows good linearity ($R^2 = 0.98$), and the estimated LOD for calcium from our LIBS measurements is found to be ~0.17 ± 0.04 µg which indicates a 5-fold improvement over calcium detection from the assay.

4. Conclusion

In this study, we established a significant milestone in using LIBS as an analytical tool for quantitative *in-vitro* detection of small amounts of calcium in cellular samples that are undetectable by conventional methods. LIBS signals for Ca emissions from analyte samples of osteogenic VICs were distinctly identified as enhancements over the corresponding signals from control cells, thereby establishing the specificity of the LIBS analysis. A linear correlation between the LIBS signal and the biochemical calcium assay results was observed that indicated a systematic increase in the Ca signals from osteogenic VICs cultured over different durations of time. While the calcium assay could significantly detect calcifications in VICs only after 7 days of culture, the LIBS results could reliably resolve Ca signals from osteogenic VICs as early as 2 days of culture. A calibration curve for the LIBS results was generated that established the LOD for quanti-

Figure 8 Linear correlation between normalized Ca signal emissions from LIBS ($I_{em, osteogenic}/I_{em, control}$) and normalized calcium content from calcium assay ($M_{Ca, osteogenic}/M_{Ca, control}$).
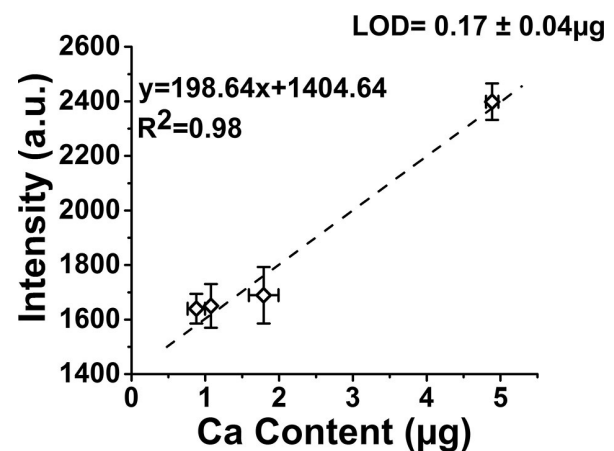
Figure 9 LIBS calibration curve for signal intensities from Ca I (422.67 nm) emission lines as a function of calcium content estimated from calcium assay LOD is estimated based on Eqn. (1). Eror bars represent mean ± std.error.

tative calcium detection to be $\sim 0.17 \pm 0.04$ μg, thereby indicating a 5-fold improvement over the conventional calcium assay measurements. Our results indicate that LIBS provides significantly lower LOD over calcium assay and histology techniques. In future, such studies may aid the fundamental research in the determination of the initiation point of calcification in aortic valves. The results from the present study provide a novel and accurate bioanalytical tool for measuring low amounts of calcium in cell samples for *in-vitro* pathological studies on laboratory platforms. Further investigations are required in future to assess the possibility of using LIBS for *in-vivo* applications.

Author biographies Please see Supporting Information online.

References

[1] B. R. Lindman, R. O. Bonow, C. M. Otto, Circulation research. **113**, 223–237 (2013).

[2] N. M. Rajamannan, M. Subramaniam, D. Rickard, S. R. Stock, J. Donovan, M. Springett, T. Orszulak, D. A. Fullerton, A. J. Tajik, R. O. Bonow, T. Spelsberg, Circulation. **107**, 2181–2184 (2003).

[3] R. V. Freeman, C. M. Otto, Circulation **111**, 3316–3326, (2005).

[4] E. R. Mohler, The American journal of cardiology **94**, 1396–1402 (2004).

[5] F. J. Schoen, Circulation **118**, 1864–1880 (2008).

[6] S. Masjedi, A. Amarnath, K. M. Baily, Z. Ferdous, Cardiovascular Pathology **25**, 185–194 (2016).

[7] J. N. Clark-Greuel, J. M. Connolly, E. Sorichillo, N. R. Narula, H. S. Rapoport, E. R. Mohler, J. H. Gorman, R. C. Gorman, R. J. Levy, The Annals of thoracic surgery **83**, 946–953 (2007).

[8] F. Ortolani, L. Rigonat, A. Bonetti, M. Contin, F. Tubaro, M. Rattazzi, M. Marchini, Italian Journal of Anatomy and Embryology **115**, 135–139 (2010).

[9] C. Y. Y. Yip, C. A. Simmons, Cardiovascular Pathology **20**, 177–182 (2011).

[10] X. Yang, X. Meng, X. Su, D. C. Mauchley, L. Ao, J. C. Cleveland, D. A. Fullerton, The Journal of thoracic and cardiovascular surgery **138**, 1008–1015. e1001, (2009).

[11] Z. Ferdous, H. Jo, R. M. Nerem, Cells Tissues Organs **197**, 372–383 (2013).

[12] H. Baumgartner, J. Hung, J. Bermejo, J. B. Chambers, A. Evangelista, B. P. Griffin, B. Iung, C. M. Otto, P. A. Pellikka, M. Quinones, Eae/Ase European journal of echocardiography: the journal of the Working Group on Echocardiography of the European Society of Cardiology., **10**, 1–25 (2009).

[13] S. R. Aggarwal, M.-A. Clavel, D. Messika-Zeitoun, C. Cueff, J. Malouf, P. A. Araoz, R. Mankad, H. Michelena, A. Vahanian, M. Enriquez-Sarano, Circulation: Cardiovascular Imaging. **6**, 40–47 (2013).

[14] S. Masjedi, Z. Ferdous, Cardiovascular engineering and technology **6**, 209–219 (2015).

[15] K. Balachandran, P. Sucosky, H. Jo, A. P. Yoganathan, Am J Pathol. **177**, 49–57 (2010).

[16] S. Bertazzo, E. Gentleman, K. L. Cloyd, A. H. Chester, M. H. Yacoub, M. M. Stevens, Nat Mater. **12**, 576–583 (2013).

[17] J. M. Connolly, I. Alferiev, J. N. Clark-Gruel, N. Eidelman, M. Sacks, E. Palmatory, A. Kronsteiner, S. Defelice, J. Xu, R. Ohri, N. Narula, N. Vyavahare, R. J. Levy, Am J Pathol. **166**, 1–13 (2005).

[18] J. A. Benton, H. B. Kern, K. S. Anseth, J Heart Valve Dis. **17**, 689–699 (2008).

[19] R. Rocha, A. B. Villaverde, C. A. Pasqualucci, L. Silveira, M. S. Costa, M. T. T. Pacheco, Photomed Laser Surg. **25**, 287–290 (2007).

[20] V. Dritsa, K. Pissaridi, E. Koutoulakis, I. Mamarelis, C. Kotoulas, J. Anastassopoulou, In Vivo **28**, 91–98 (2014).

[21] N. Vyavahare, D. Hirsch, E. Lerner, J. Z. Baskin, F. J. Schoen, R. Bianco, H. S. Kruth, R. Zand, R. J. Levy, Circulation **95**, 479–488 (1997).

[22] M. A. Bowler, W. D. Merryman, Cardiovasc Pathol. **24**, 1–10 (2015).

[23] L. J. Radziemski, D. A. Cremers, in: *Spectrochemical analysis using laser plasma excitation*, Marcel Dekker Inc., New York, NY, USA (1989).

[24] D. W. Hahn, N. Omenetto, Appl Spectrosc. **66**, 347–419 (2012).

[25] D. Mukherjee, A. Rai, M. R. Zachariah, J Aerosol Sci. **37**, 677–695 (2006) .

[26] F. Ferioli, S. G. Buckley, Combust Flame **144**, 435–447 (2006).

[27] A. E. Majd, A. S. Arabanian, R. Massudi, M. Nazeri, Appl Spectrosc. **65**, 36–42 (2011).

[28] F. Ferioli, P. V. Puzinauskas, S. G. Buckley, Applied Spectroscopy **57**, 1183–1189 (2003).

[29] R. Wisbrun, I. Schechter, R. Niessner, H. Schroder, K. L. Kompa, Anal Chem. **66**, 2964–2975 (1994).

[30] D. A. Cremers, M. H. Ebinger, D. D. Breshears, P. J. Unkefer, S. A. Kammerdiener, M. J. Ferris, K. M. Catlett, J. R. Brown, J Environ Qual. **30**, 2202–2206 (2001).

[31] D. Mukherjee, M. D. Cheng, Journal of Analytical Atomic Spectrometry **23**, 119–128 (2008).

[32] J. L. Gottfried, Analytical and Bioanalytical Chemistry **400**, 3289–3301 (2011).

[33] J. L. Gottfried, F. C. De Lucia, C. A. Munson, A. W. Miziolek, Applied Spectroscopy **62**, 353–363 (2008).

[34] B. E. Naes, S. Umpierrez, S. Ryland, C. Barnett, J. R. Almirall, Spectrochim Acta B **63**, 1145–1150 (2008).

[35] J. L. Gottfried, Applied Optics **52**, B10–B19 (2013).

[36] F. C. De Lucia, J. L. Gottfried, Journal of Physical Chemistry A **117**, 9555–9563 (2013).

[37] J. L. Gottfried, F. C. De Lucia, C. A. Munson, A. W. Miziolek, Analytical and Bioanalytical Chemistry **395**, 283–300 (2009).

[38] D. Mukherjee, M. D. Cheng, Applied Spectroscopy **62**, 554–562, (2008).

[39] L. St-Onge, E. Kwong, M. Sabsabi, E. B. Vadas, Spectrochim Acta B **57**, 1131–1140 (2002).

[40] A. Kumar, F. Y. Yueh, J. P. Singh, S. Burgess, Applied Optics **43**, 5399–5403 (2004).

[41] V. K. Singh, A. K. Rai, Laser Med Sci. **26**, 307–315 (2011).

[42] S. A. Davari, S. Hu, D. Mukherjee, Talanta **164**, 330–340 (2017).

[43] J. D. Hybl, G. A. Lithgow, S. G. Buckley, Appl Spectrosc. **57**, 1207–1215 (2003).

[44] F. Mehari, M. Rohde, C. Knipfer, R. Kanawade, F. Klampfl, W. Adler, N. Oetter, F. Stelzle, M. Schmidt, Plasma Sci Technol. **18**, 654–660 (2016).

[45] O. Samek, D. C. S. Beddows, H. H. Telle, J. Kaiser, M. Liska, J. O. Caceres, A. G. Urena, Spectrochimica Acta Part B-Atomic Spectroscopy **56**, 865–875 (2001).

[46] V. K. Singh, V. Kumar, J. Sharma, Lasers in Medical Science **30**, 1763–1778 (2015).

[47] S. Masjedi, Y. Lei, J. Patel, Z. Ferdous, Heart and vessels **32**, 217–228 (2017). doi:10.1007/s00380-016-0909-8 (2016).

[48] A. Kramida, Ralchenko, Yu., Reader, J. and NIST ASD Team in NIST Atomic Spectra Database (version 5.3), National Institute of Standards and Technology, Gaithersburg, MD (2015).

[49] K. Seya, Z. Yu, K. Kanemaru, K. Daitoku, Y. Akemoto, H. Shibuya, I. Fukuda, K. Okumura, S. Motomura, K. Furukawa, Journal of pharmacological sciences **115**, 8–14 (2011).

[50] H. L. Holtorf, J. A. Jansen, A. G. Mikos, J Biomed Mater Res A **72**, 326–334 (2005).

[51] C. H. Byon, A. Javed, Q. Dai, J. C. Kappes, T. L. Clemens, V. M. Darley-Usmar, J. M. McDonald, Y. Chen J Biol Chem. **283**, 15319–15327 (2008).

[52] Y. M. Kolambkar, A. Peister, A. K. Ekaputra, D. W. Hutmacher, R. E. Guldberg, Tissue Eng Part A **16**, 3219–3230 (2010).

FULL ARTICLE
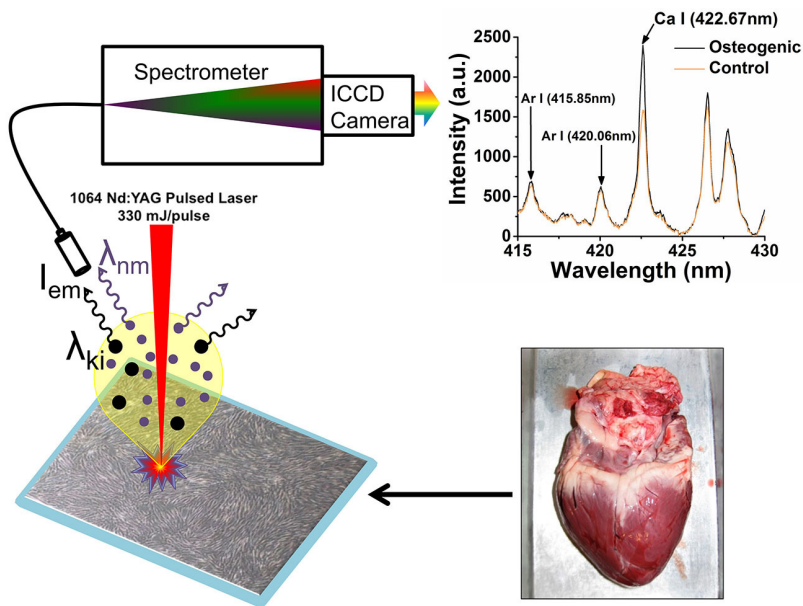
S. A. Davari, S. Masjedi, Z. Ferdous, D. Mukherjee*

1 – 10

In-vitro analysis of early calcification in aortic valvular interstitial cells using Laser-Induced Breakdown Spectroscopy (LIBS)

Quantitative LIBS enables *in-vitro* analysis for early stage detection of calcium deposition within aortic valvular interstitial cells (VIC).